8086–8096 *Nucleic Acids Research, 2016, Vol. 44, No. 17* *Published online 24 May 2016*
doi: 10.1093/nar/gkw464

Preferential extension of short telomeres induced by low extracellular pH

Yuanlong Ge[1,2,3,†], Shu Wu[1,†], Yong Xue[4], Jun Tao[5], Feng Li[1], Yanlian Chen[1,2], Haiying Liu[1,2], Wenbin Ma[1], Junjiu Huang[1] and Yong Zhao[1,2,*]

[1]Key Laboratory of Gene Engineering of the Ministry of Education, State Key Laboratory of Biocontrol, School of Life Sciences, Sun Yat-sen University, Guangzhou 510006, China, [2]Collaborative Innovation Center of High Performance Computing, National University of Defense Technology, Changsha 410073, China, [3]Zhongshan Medical School, Sun Yat-sen University, Guangzhou 510006, P. R.China, [4]Jiangsu Key Laboratory of Marine Pharmaceutical Compound Screening, Huaihai Institute of Technology, Lianyungang 222005, China and [5]Department of Hypertension and Vascular Disease, The First Affiliated Hospital, Sun Yat-Sen University, Guangzhou 510006, China

Received June 21, 2015; Revised May 14, 2016; Accepted May 17, 2016

ABSTRACT

The majority of tumor cells overcome proliferative limit by expressing telomerase. Whether or not telomerase preferentially extends the shortest telomeres is still under debate. When human cancer cells are cultured at neutral pH, telomerase extends telomeres in telomere length-independent manner. However, the microenvironment of tumor is slightly acidic, and it is not yet known how this influences telomerase action. Here, we examine telomere length homeostasis in tumor cells cultured at pHe 6.8. The results indicate that telomerase preferentially extends short telomeres, such that telomere length distribution narrows and telomeres become nearly uniform in size. After growth at pHe 6.8, the expression of telomerase, TRF1, TRF2 and TIN2 decreases, and the abundance of Cajal bodies decreases. Therefore, telomerase are insufficient for extending every telomere and shorter telomeres bearing less shelterin proteins are more accessible for telomerase recruitment. The findings support the 'protein-counting mechanism' in which extended and unextended state of telomere is determined by the number of associated shelterin proteins and the abundance of telomerase. Decreased expression of telomerase and preferential extension of short telomeres have important implications for tumor cell viability, and generate a strong rationale for research on telomerase-targeted anti-cancer therapeutics.

INTRODUCTION

The microenvironment of tumors is characterized by oxygen deficiency (hypoxia) due to structural and functional inadequacy of the vasculature that delivers oxygen and other nutrients to the tumor cells (1). As a result, tumor cells depend on processing glucose through the glycolytic pathway, to generate pyruvate and lactic acid, a phenomenon called the Warburg effect (2–3). High dependence on glycolysis generates excess hydrogen ions (H^+), which acidifies the extracellular environment in the tumor (4–5). The pH of the extracellular space has been measured directly in human tissues by insertion of electrode or nuclear magnetic resonance probes (6–8). These studies showed that the extracellular pH (pHe) of normal and cancer cells was ∼7.4 and 6.9, respectively. The acidic extracellular microenvironment of tumor cells correlates with altered gene expression, and is thought to facilitate tumorigenic transformation, tumor cell migration and invasion (9).

DNA replicative enzymes are incapable of replicating the terminal segment of eukaryotic chromosomes (end replication problem), such that chromosomal telomeres grow progressively shorter when telomerase is absent. Eventually, extremely short telomere induces replicative senescence or apoptosis (10). Many cancer cells avoid replicative senescence by expressing active telomerase, a ribonucleoprotein with reverse transcriptase activity that adds telomeric GGTTAG sequence to the end of telomeres (11). Therefore, telomerase is considered as a potential target for cancer therapeutics, and it is important to understand how telomerase extends telomeres in human cancer cells. One model proposes that telomerase preferentially extends the shortest telomeres in mammalian cells under the situation in which either telomerase or telomere length was artificially changed (12–15), whereas under telomere length maintenance condition, telomerase extends telomeres in a length-independent

*To whom correspondence should be addressed. Tel: +86 203 994 3401; Fax: +86 203 933 2944; Email: zhaoy82@mail.sysu.edu.cn
† These authors contributed equally to the paper as first authors.

manner (16,17). To date, no studies have examined how the acidic extracellular pH of tumor microenvironment influences telomere extension by telomerase.

Protein factor that modulates telomere extension by telomerase is a six-protein telomere binding complex called 'shelterin' (18). Shelterin components negatively regulate telomerase (12). For instance, overexpression of shelterin protein, TRF1 or TRF2, causes progressive shortening of telomeres in human cancer cells (19) and knockdown of other shelterin protein, TIN2 or TPP1 or POT1 in telomerase-positive cells leads to telomere elongation (20–22). The shelterin complex may inhibit telomerase by physically blocking accessibility to the telomeres (12). It has been proposed that yeast cells and possibly human cells can physically 'count' the number of shelterin molecules per telomere, and that the higher number, the lower potential of that telomere to be extended by telomerase. This is called the 'protein-counting mechanism', but it is not understood in molecular detail how shelterin molecules are detected and 'counted', or how telomerase is selectively inhibited from extending longer telomeres. Nevertheless, it is clear that a protein-counting mechanism does not apply when human tumor cells are grown at pHe 7.4 (16). As mentioned above, no published data addresses the question of whether a protein-counting mechanism exists to target telomerase to short telomeres in tumor cells cultured in a slightly acidic microenvironment.

This study compares telomere extension in tumor cells cultured in medium at pHe 6.8 and pHe 7.4. The results show that longer telomeres become progressively shorter and shorter telomeres become longer, such that the size distribution narrows over successive generations of cells grown at pHe 6.8. These and other data support the hypothesis that telomerase selectively extends short telomeres when the extracellular pH is slightly acidic. Furthermore, the abundance of telomerase protein, the number of Cajal bodies, which deliver telomerase to telomeres, and the abundance of TRF1/TRF2/TIN2 decreases under slightly acidic growth conditions. These results suggest that the protein-counting mechanism selectively targets active telomerase to short telomeres in human tumor cells. The implications of these results are discussed.

MATERIALS AND METHODS

Cell culture

HeLa cells were obtained from Cell Resource Center of Peking Union Medical College and were cultured at 37°C under 5% CO_2 in Dulbecco's modified Eagle's medium (DMEM) (Sigma) supplemented with 10% fetal calf serum (PAA) and 100U/ml penicillin and streptomycin (HyClone). The pH of DMEM was adjusted as previously described (23). Briefly, the appropriate amount of bicarbonate and HEPES were added to DMEM to adjust pH to 6.8, 7.1 or 7.4. The pH of final media was measured after 5% CO_2 was bubbled into medium for 30 min. The pH of medium was measured intermittently during cell culture. The data show that media pH changed less than 0.2 units on average during the course of experiment.

Cell cycle synchronization

Exponentially growing HeLa cells were synchronized with thymidine (2 mM) for 19 h, washed with pre-warmed phosphate buffered saline (PBS) (three times), then incubated with fresh medium for 9 h. Thymine (2 mM) was added to medium and cells were incubated for additional 17 h before released into fresh medium.

Telomere restriction fragment (TRF) assay

Genomic DNA was extracted using AxyPrepTM Blood Genomic DNA Miniprep Kit (Axygen Biosciences, Union City, USA) following the instruction provide by manufacture. Isolated DNAs were digested with Hinf I and Rsa I and resolved on a 0.7% agarose gel. The denatured and dried gel was hybridized with ^{32}P-labeled oligonucleotides $(TTAGGG)_4$ and exposed to a PhosphorImager screen. The weighted mean telomere length was calculated as described previously (13).

TRAP assay

TRAP (Telomeric Repeat Amplification Protocol) assay was performed as described previously (11). The telomerase products (6 bp ladder) and the 36 bp internal control (IC) bands were quantified using the ImageQuant (GE). Relative telomerase activity was calculated as the intensity ratio of TRAP ladders to IC band.

Fluorescence *insitu* hybridization (FISH) and immunofluorescence (IF) assay of TRF2 and/or coilin

Fluorescence *in situ* hybridization (FISH) and immunofluorescence (IF) were performed as previously described (24). Briefly, cells on coverslip were fixed with 4% paraformaldehyde, permeablized in 0.5% Triton X-100 (in 1 × PBS). Cells were incubated overnight at 4°C with primary antibodies against coilin (Abcam) or TRF2 (Millipore) or 53BP1(Novus), washed three times, and incubated with secondary antibodies (DyLight 488-conjugated anti-mouse or DyLight 405-conjugated anti-rabbit). The cover slip was washed with PBS, incubated in 4% paraformaldehyde for 10 min, washed in ethanol series solutions, denatured at 85°C for 3–5 min, and then hybridized with Cy3-labeled $(CCCTAA)_3$ PNA probe (Panagene) at 37°C for 2 h. The cells was washed and mounted with DAPI. Fluorescence was detected and imaged using Nikon Ti microscope. The fluorescence intensity of telomeres was analyzed by Image J software. To quantify the relative length of telomeres occupied by Cajal bodies (Telomeres that colocalize with coilin foci), over 700 cells from each group (pH 7.4 and pH 6.8) were randomly chose from three independent experiments. The group information is masked from the person examining the cells. Cajal bodies-occupied telomeres were sorted out and their size was determined by Image J software.

Isolation of BrdU-labeled nascent telomeric DNA

CsCl gradient separation of leading versus lagging telomeres was performed as previously described (16,25). CsCl fractions containing lagging telomeres were pooled together

and surface-dialyzed (2% agarose gel) to reduce the salt concentration and then precipitated by ethanol. Purified lagging telomere DNA were digested by duplex-specific nuclease (DSN) (0.5 units, Evrogen) and subjected to second round of CsCl gradient. Telomeric overhangs in each fraction were detected by slot blot and hybridization with telomeric C-rich probe. The overhang signal of each fraction was plotted with corresponding density of CsCl. Obtained curve was fitted with the function of Two Gaussians Distributions and areas of Gaussian peaks were calculated using Prism 5 (GraphPad Software, Inc.).

In gel hybridization to determine the relative abundance of telomeric overhangs

Isolated genomic DNAs were digested with Hinf1 and RsaI and resolved on a 0.7% agarose gel. DNA digested with 10 U of exonuclease I (NEB) served as a control (background). The gel was dried, prehybridized (6 × SSC, 5 × Denhardt's solution, 0.5% [w/v] sodium dodecyl sulphate (SDS)) and hybridized with C-rich probe under a native condition. Gel was exposed to a PhosphorImager screen and the signal of telomeric overhangs was obtained by scanning at Typhoon Scanner (GE). The gel was then denatured (0.5 M NaOH, 1.5 M NaCl for 1 h), rinsed three times with distilled water, neutralized (0.5M Tris–HCl at pH 8, 1.5M NaCl for 30 min) and re-hybridized with C-rich probe. Thus, the signal of total telomeres was obtained by exposing gel to PhosphorImager followed by scanning at Typhoon Scanner (GE). The relative abundance of telomeric overhangs was calculated by normalizing the signal of telomeric overhangs to the signal of total telomeres.

To determine the net increase in overhang abundance from 0 h (G1/S) to 6 h (late S phase) for telomeres of different length, telomeres resolved on gel were divided into 90 intervals according to their size. The relative overhang signal at each interval was determined as described above. Net increase was calculated by subtracting overhang signal at 0 h (before telomerase action) from overhang signal at 6 h (after telomerase action but before C-rich Fill-in). The net increase of overhang abundance in intervals corresponding to telomere size from N − 0.5 to N + 0.5 kb ($N = 1, 2, 3\ldots$) were added up and the sum was plotted with size N kb using Prism 5 (GraphPad Software, Inc.).

Telomere quantitative fluorescent in situ hybridization (Q-FISH)

Q-FISH was performed as previously described (26). FITC-labeled $(CCCTAA)_3$ PNA probe (Panagene, Korea) was used. Fluorescence of telomeres was digitally imaged on a Zeiss microscope with FITC/DAPI filters. The fluorescence intensity of telomeres was analyzed by AxioVision software 4.8 and TFL-TELO program (a gift from P. Lansdorp).

Western blot

Cell samples were lysed and boiled for 10 min. Proteins were separated by sodium dodecyl sulphate-polyacrylamide gel electrophoresis, transferred to PVDF membrane and detected with relevant antibodies against TRF1 (GeneTex), TRF2 (Millipore), RAP1(Proteintech), coilin (Abcam), H4ac (Millipore) or H3K9ac (Sigma).

Chromatin immunoprecipitation (ChIP)

Cells were cross-linked with 1% formaldehyde for 10 min at room temperature and washed twice with cold PBS, resuspended in SDS lysis buffer (50mM Tris–HCl, pH = 8.1, 10 mM ethylenediaminetetraacetic acid, 1% SDS) and sonicated to fragments of 200 bp to 1 kb. The supernatant was pre-cleared with Protein-A agarose beads precoated with *Escherichia coli* genomic DNA. Chromatin immunoprecipitation (ChIP) was carried out overnight at 4°C with anti-TRF2 (Millipore), anti-H3K9ac (Sigma), anti-H4ac (Millipore) or IgG (Sangon). Beads were washed three times, and eluted with 0.1M $NaHCO_3$ & 1% SDS, followed by reverse cross-linking and phenol-chloroform extraction. DNA fragments were precipitated by ethanol and blotted onto NC membranes. Telomeric DNA was detected by hybridization with telomere-specific probe.

Quantitative real-time PCR

Total RNA was extracted from cells using RNAiso Plus Reagent (Takara) according to manufacturer's instructions. Total RNA (1.0 μg) was reverse-transcribed to cDNA using PrimeScript RT reagent Kit (Takara). An equal amount of cDNA was used for real-time polymerase chain reaction (PCR) in Realtime PCR Master Mix (ABI). β-actin was used as an IC for all experiments. The threshold cycle (CT) value was calculated using the Step One software V2.1 provided by ABI. The following primers were used for PCR: β-actin-forward:5′-CATGTACGTTGCTATCCAGGC-3′; β-actin-reverse: 5′-CTCCTTAATGTCACGCACGAT-3′; hTERT-forward: 5′-GGAGCAAGTTGCAAAGCA TTG-3′; hTERT-reverse: 5′-CCCACGACGTAGTCCATGTT-3′; hTR-forward: 5′-AACCCTAACTGAGAAGGGCGTAGGCG-3′; hTR-reverse: 5′-GCGAACG GGCCAGCAGCTGACATT-3′; TRF1-forward: 5′-AACAGCGCAGAGG CTATTATTC-3′; TRF1-reverse: 5′-CCAAGGGTGTAATTCGTTCATCA-3′; TRF2-forward: 5′-GTACGGGGACTTCAGACAGAT-3′; TRF2-reverse: 5′- CGCGACAGACACTGCATAAC-3′; RAP1-forward: 5′-GCGTCTGGTCA GAGAGCTG-3′; RAP1-reverse: 5′-TCAATCCTCCGAGCTACATTCT-3′; TIN2-forward: 5′-ACGCCTTTGTATGGGCCTAAA-3′; TIN2-reverse: 5′-AAGTTTCCTGTGCCTCCAAAAT-3′; POT1-forward: 5′-CAGCCAATGCA GTATTTTGACC-3′; POT1-reverse: 5′-GGTGCCATCCCATACCTTTAGAA-3′; TPP1-forward: 5′-CCTCCACACGGTGCAAAAATG-3′; TPP1-reverse: 5′- CTCTGCTTGTCGGATGCTCAG -3′.

RNA&DNA FISH

RNA&DNA FISH was performed to detect hTR and telomeres as described previously (27) with a minor modification. Briefly, S phase-synchronized cells were fixed with 4% paraformaldehyde for 30 min at room temperature, permeablized in 0.1% Triton X-100 (in 1×PBS). Cells were

then blocked with prehybridization buffer at 37°C for 1h and denatured at 85°C for 5 min. Hybridization was carried out in hybridization buffer containing both hTR probe (fluorescein isothiocyanate-conjugated DNA probes complementary to hTR (28)) (TAKARA Bio Inc) and telomeric probe (Cy3-labeled $(CCCTAA)_3$) (Panagene, Korea) at 37°C overnight. Cells were then washed and mounted with DAPI. Fluorescence was detected and imaged using Nikon Ti microscope.

Micrococcal nuclease assay

Micrococcal nuclease assay was performed as previously described (29).

Statistical analysis

The student's two-tailed unpaired *t*-test was used to determine statistical significance and the resulting *P*-values are indicated in figures.

RESULTS

Reduced length and heterogeneity of telomeres in cells cultured at pHe 6.8

A previous *in vivo* study demonstrated that the extracellular pH (pHe) of tumors was in the range of 6.7–7.1 (30), while the pHe of normal human cells was 7.4. To examine how pHe influences cell growth and telomere homeostasis, tumor cells were cultured at pHe 6.8, 7.1 and 7.4, rates of cell proliferation, apoptosis and senescence were evaluated, and telomere properties were analyzed. The results show that cells cultured at pHe 7.1 or 7.4 proliferate at a similar rate, while cells cultured at pHe 6.8 proliferate slowly (Figure 1A). No senescent or apoptotic cells were observed (data not shown). After 30 population doublings (PDs), we used the telomere restriction fragment (TRF) method to measure telomere length. Cells cultured at pHe 7.4 demonstrated typical heterogeneity (2–12 kb) and average length of telomeres (5.4 kb), and the telomere length distribution was maintained through 30 PDs (Figure 1B). In contrast, cells cultured at pHe 6.8 displayed progressive shortening of longer telomeres and progressive lengthening of shorter telomeres. Through ∼20 PDs, the length of telomeric restriction fragments became considerably less heterogeneous and the distribution of telomere lengths narrowed; for the last 10 PDs, the new more uniform telomere length distribution was maintained (Figure 1B).

In the above experiment, the average telomere length in a population of cells was measured by the TRF assay. To evaluate telomere lengths at the single cell level, telomeres in a single cell were visualized by q-FISH and their sizes were compared for cells grown at pHe 6.8 for 0 PD and 33 PDs. In the PD = 0 cell, telomere length ($n = 285$) was heterogeneous, ranging from 60 to 500 relative telomere length (RTL). However, after 33 PDs at pHe 6.8, telomere length ($n = 270$) ranged from 80 to 280 RTL (Figure 1C and D), indicating decreased length and heterogeneity at the single cell level. Similar results were obtained with a larger q-FISH sample size (cell population) of 15 321 telomeres of PD = 0 cells and 11552 telomeres of PD = 33 cells (Figure 1E). These results strongly suggest that telomerase selectively extends short telomeres in tumor cells grown at pHe 6.8.

Detection of nascent DNA on short telomeres at pHe 6.8

Previous studies using HeLa cells cultured at pHe 7.4 suggest that during S phase of cell cycle, telomerase adds ∼60 nt of the telomeric repeat (GGTTAG) to almost each telomere in cell in a telomere length-independent manner (16). Results presented in Figure 1 show that long telomeres shorten progressively at pHe 6.8. As mentioned above, a possible explanation for that result is selective extension of short telomeres by telomerase. To explore this possibility, we first determined the percentage of telomeres that were extended by telomerase during one cell cycle. During telomere replication of lagging daughter, the parental G-rich strand does not incorporate BrdU, so the overhangs remain unlabeled and of low density until they are extended by telomerase (Figure 2A). By counting the number of lagging overhangs with (extended, higher density) and without BrdU (unextended, low density), the fraction of telomere ends extended by telomerase can be determined (Figure 2A). For this experiment, HeLa cells were cultured in medium containing BrdU for one cell cycle (20 h for pHe 7.4 and 30 h for pHe 6.8). Genomic DNA was harvested and lagging daughter of telomeres was isolated by CsCl density-gradient centrifugation (Supplementary Figure S1). The recovered lagging telomeres were digested with DSN and subjected to a second round of CsCl density gradient centrifugation. The fraction of telomeric overhangs of high and low density was measured by slot blot and fitted to Gaussian distributions (16); the ratio of overhangs with high density indicates the fraction of telomeres extended by telomerase during one cell cycle (Figure 2A). The results showed that telomerase extended 77 ± 4% of telomeres at pHe 7.4, consistent with our previous report (16). However, only 48 ± 4% of telomere ends were extended by telomerase when cells were cultured at pHe 6.8 (Figure 2B and C).

To further understand how telomerase acts upon different length telomeres, we examined the change of overhang length during S phase using in-gel hybridization. Because telomere extension by telomerase and C-rich fill-in are uncoupled, 3′ overhangs are transiently longer during S phase (16). This makes it possible to measure and compare the increases of telomere overhang length during S phase in cells cultured at pHe 7.4 or pHe 6.8. For this experiment, cells were synchronized at G1/S, released into S phase for 6 h (just before C-rich fill-in) and harvested (Supplementary Figure S2). Genomic DNA was isolated and telomeric DNA was electrophoresed into a 0.7% agarose gel. Electrophoresis was stopped after telomeres had penetrated ∼1 cm into the gel so that telomeres of various lengths did not separate significantly according to size but remained as a compact hand that concentrated the overhang signal into a small area. Relative overhang abundance on telomeres was determined by in gel hybridization, in which the signal hybridizing to the overhang (native) is compared to the total telomere signal following denaturation (Figure 2D). As expected, quantitative results showed the increase of overhang abundance at late S phase (6 h after release) for cells cultured at pHe 6.8 and 7.4, demonstrating the extension

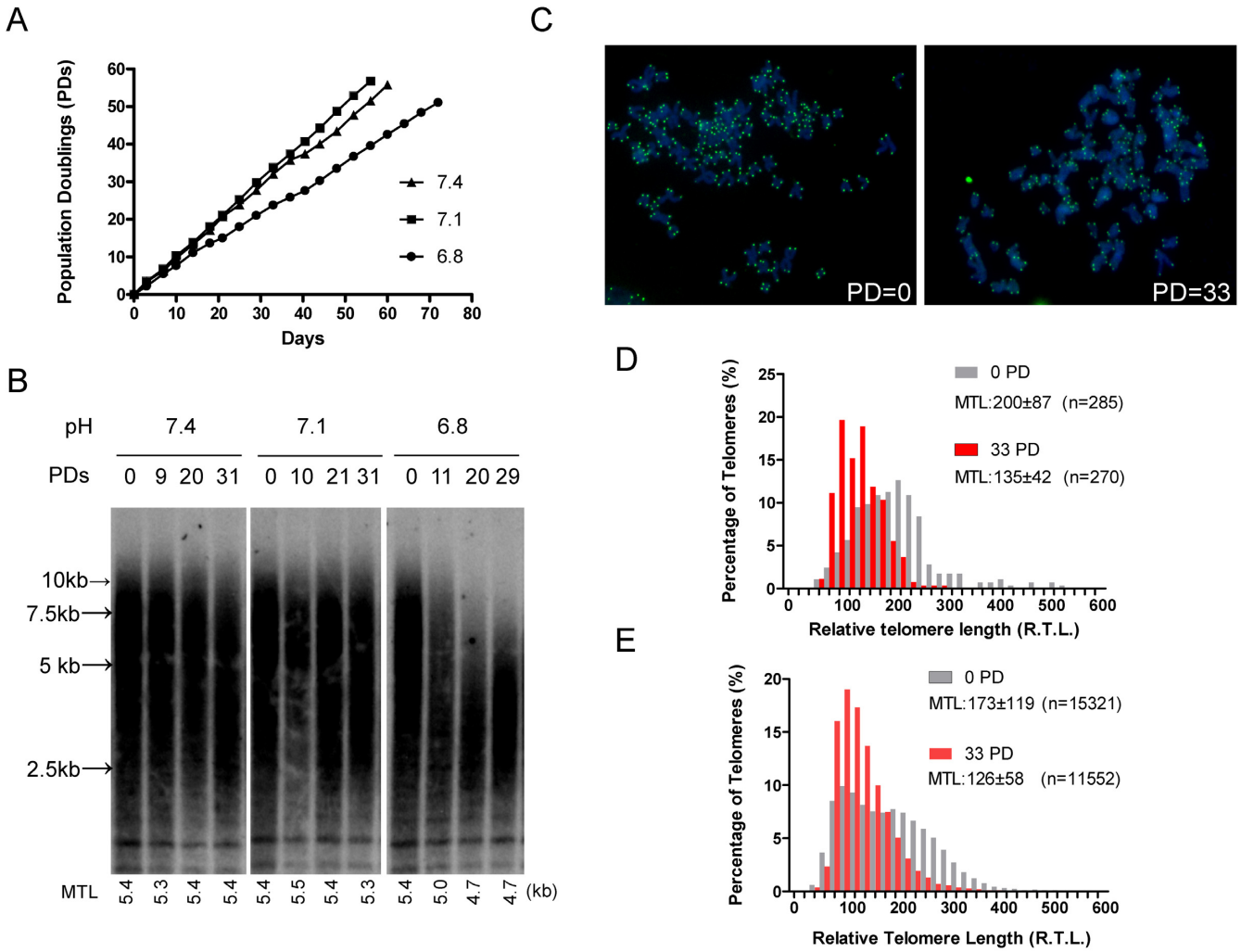

Figure 1. Homogenous telomere length of HeLa cells after long-term culture at pHe 6.8. (**A**) Growth curves of cells cultured in medium with indicated pHe. (**B**) Cells were cultured at the indicated pHe for ∼30 PDs, and telomere length was determined by TRF assay. (**C**) Q-FISH assay to determine telomere length in cells at PD = 0 and PD = 33; cells were cultured at pHe 6.8. A typical image is shown. (**D**) Quantification of panel C: telomeres in single cell at PD = 0 ($n = 285$) and at PD = 33 ($n = 270$). (**E**) Quantification of telomere length of cell population grown at pHe 6.8 for 0 and 33 PDs ($n = 15\,321$ for PD = 0; $n = 11\,552$ for PD = 33). MTL: Mean Telomere Length.

of overhang by telomerase. However, the relative overhang abundance of cells cultured at pHe 6.8 is slightly less than that of cells cultured at pHe 7.4 ($P = 0.027$), indicating less extension occurring on telomeres in cells grown at pHe 6.8.

Given the fact that telomeres extended by telomerase have longer overhang during S phase and that only 48% of telomeres are extended by telomerase in cells cultured at pHe 6.8 (Figure 2B and C), the purpose of following experiment is to determine which telomeres (long or short telomeres) are extended by telomerase: telomeres were fully resolved by size by agarose gel electrophoresis; telomeres on gel were divided into 90 intervals according to their size, so each interval corresponds to the cohort of telomeres with a specific size; relative overhang abundance and net increase from 0 h (G1/S) to 6 h (late S phase) in each interval was calculated by in gel hybridization overhang assay (Figure 2E, see 'Materials and Methods' section for details). Figure 2F shows a graph of the net increase of overhang abundance for telomeres of different length. The results show that telomere extension as indicted by increased abundance of overhangs was relatively insensitive to telomere length over the range 2–10 kb in cells grown at pHe 7.4, while in contrast, there was selective or preferential extension of short telomeres in cells grown at pHe 6.8.

Decreased abundance of telomerase in cells cultured at pH 6.8

One possible mechanism for preferential extension of short telomeres at low pHe is decreased abundance of telomerase. Therefore, the abundance of hTR and hTERT was determined by q-PCR. Although no difference in hTR level was observed, expression of hTERT was ∼50% lower in cells cultured at pHe 6.8 than in cells cultured at pHe 7.4 (Figure 3A). Consistent with this result, *in vitro* TRAP assay (Figure 3B and C) showed that telomerase activity was ∼50% lower in cells grown at pHe 6.8. However, when hTERT shRNA was used to reduce the level of hTERT mRNA in HeLa

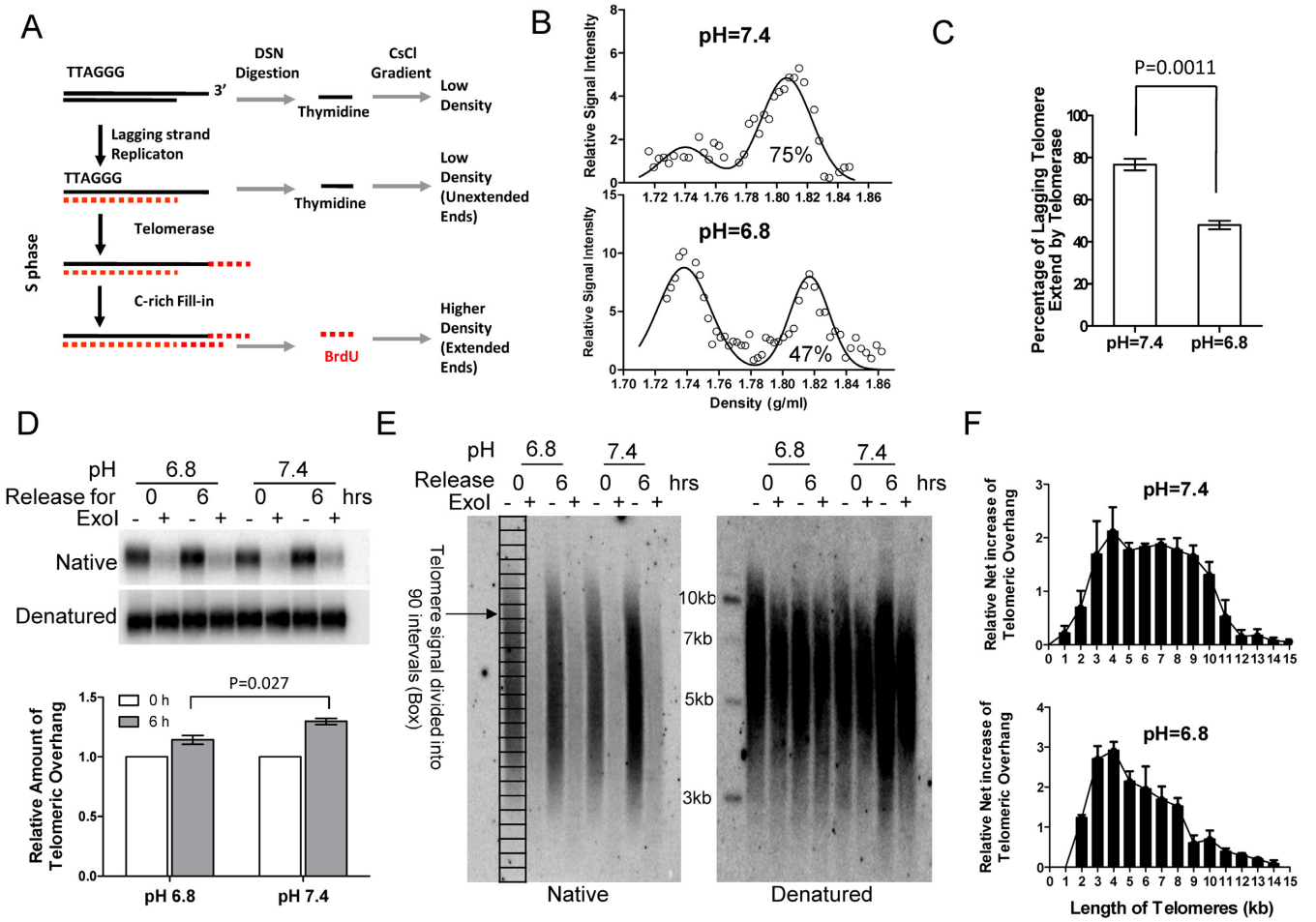

Figure 2. Telomerase selectively extends short telomeres in cells cultured at pHe 6.8. (**A**) Diagram of experimental method for studying telomere extension on lagging daughter telomeres. Lagging daughter telomeres are first isolated by CsCl gradient, and then subjected to DSN digestion and second round of CsCl gradient. Extended overhangs but not unextended overhangs incorporate BrdU, resulting in increase in density. (**B**) About 75% lagging overhangs are extended by telomerase at pHe 7.4, and 47% lagging overhangs are extended at pHe 6.8. Cells grown at pHe 7.4 and 6.8 were exposed to BrdU (100 μM in medium) for 20 and 30 h, respectively. The genomic DNA was then purified and subjected to overhang assay by CsCl gradient. (**C**) Quantification of B, Values are average ±SD of three independent experiments. *P*-value was calculated using the Student's *t*-test. (**D**) In gel hybridization assay to determine the relative overhang abundance in cells at G1/S (0 h, before telomerase action) and late S/G2 (6 h, after telomerase extension but before C-rich Fill-in). Cells cultured at indicated pHe were synchronized at G1/S and released into S phase for 6 h. Values are average ±SD of three independent experiments. *P*-value was calculated using the Student's *t*-test. (**E**) In gel hybridization assay to determine the net increase of overhang abundance for telomeres of different size (6 over 0 h during S phase). Telomeres on gel were divided into 90 intervals according to size. Symbolistic grid for dividing telomere signal was shown. (**F**) Quantification of E, values are average ±SD of three independent experiments. Relative net increase of overhang abundance of intervals (6 over 0 h) was plotted with corresponding telomere size (see 'Materials and Methods' section for details). The pHe of culture medium is indicated.

cells to ∼50% of normal level (Figure 3D and Supplementary Figure S3), telomere shortening occurred over 30 PDs in a length-independent manner, when cells were grown at pHe 7.4 (Figure 3E). The conclusion was further confirmed by q-FISH assay in which telomere length of telomerase-deficient cells (clone 7) at early (5 PD, $n = 6012$) and late PDs (30 PD, $n = 5066$) were compared (Figure 3F and G). Thus, decreased abundance of telomerase is not sufficient for preferential extension of short telomeres.

Histone acetylation at telomeric chromatin and decreased abundance of shelterin complex

Previous studies reported decreased histone acetylation when tumor cells were cultured at acidic pHe (23) and that altered telomeric epigenetic marks correlate with telomere length deregulation (31–32). To explore whether histone acetylation varies with pHe, the abundance of acetylated telomeric histones was measured in cells cultured at pHe 7.4 or 6.8 using a ChIP assay. The results showed that the abundance of acetylated histones in telomeric chromatin was independent of pHe for HeLa cells grown in culture at pHe 7.4 or 6.8 (Supplementary Figure S4A and B). Consistent with this observation, micrococcal nuclease (MNase) assay showed that the extent of condensation/decondensation of telomeric DNA was also independent of pHe (Supplementary Figure S4C and D). These results rule out the possibility that pHe-dependent changes in telomeric heterochromatin regulate telomerase, leading to preferential extension of short telomeres.

The abundance of mRNAs encoding shelterin components TRF1, TRF2, RAP1, TIN2, POT1 and TPP1 was

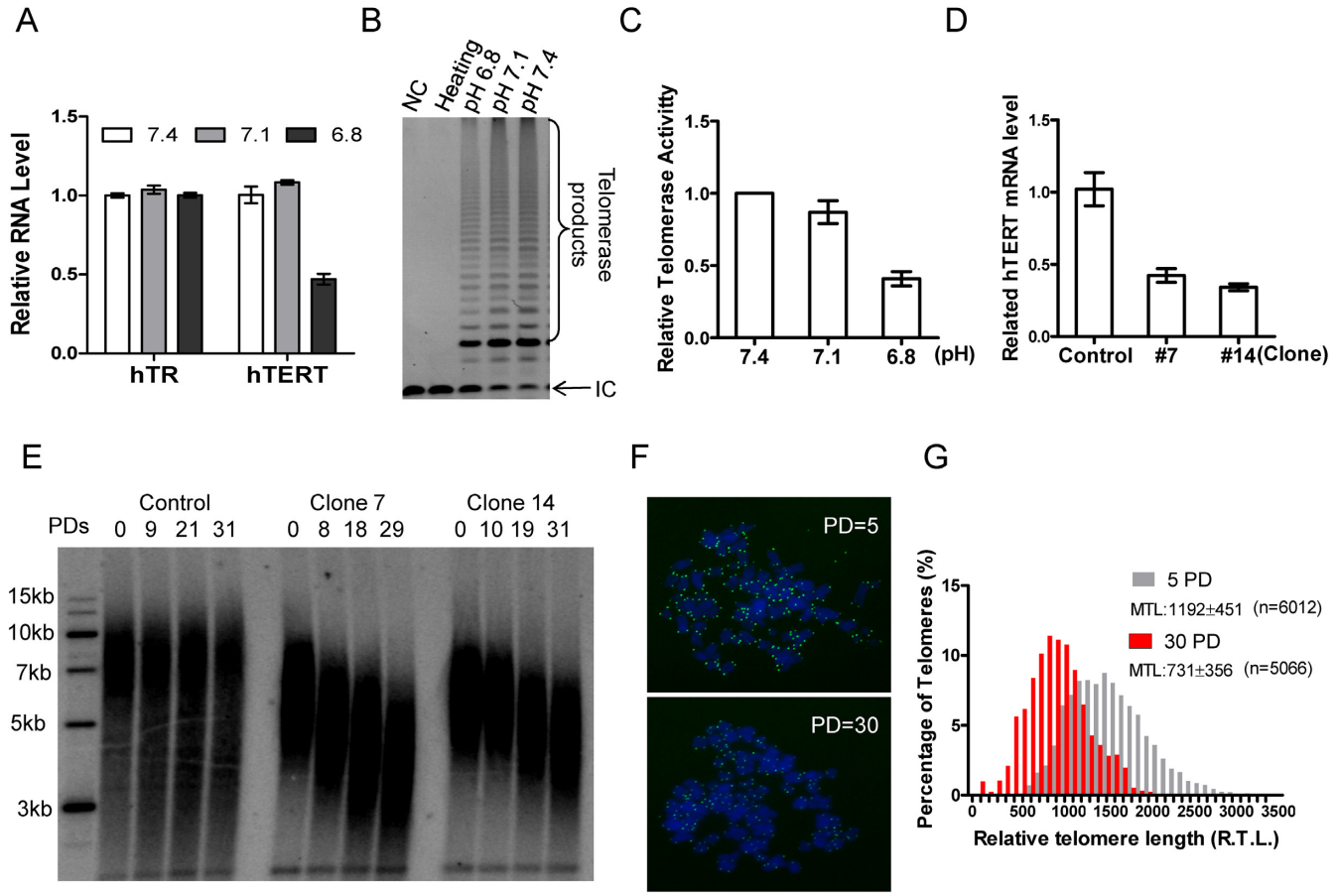

Figure 3. Decreased expression of telomerase in cells cultured at pHe 6.8. (**A**) RNA was quantified by q-PCR. Values are average ±SD of three independent experiments. (**B**) TRAP assay for telomerase activity in cells cultured at the indicated pHe. Cell extract equal to 50 cells were used for the assay. (**C**) Quantification of (B); values are average ±SD of three independent experiments. (**D**) Relative abundance of hTERT mRNA was measured by q-PCR for clone 7 and clone 14 cells in which hTERT is knocked down by shRNA. (**E**) TRF assay of cells cultured for the indicated number of PDs. (**F**) q-FISH to determine telomere length in clone 7 cells cultured for indicated PDs. (**G**) Quantification of F ($n = 6012$ for PD = 5; $n = 5066$ for PD = 30). MTL: Mean Telomere Length.

also determined by q-PCR. The results showed a significant decrease in expression of TRF1, TRF2 and TIN2 at pHe 6.8 (Figure 4A). Western blot analysis confirmed decreased abundance of TRF1 and TRF2 protein at pHe 6.8 (Figure 4B). Antibody against TRF2 was validated by knockdown experiment using CRISPR/Cas9-based technique (Supplementary Figure S5). Because TRF1 and TRF2 associate directly with telomeric dsDNA (18), we examined whether low pHe leads to reduced coating of telomeres by the shelterin complex using IF with antibody to TRF2 and FISH assay for telomere repeats, respectively. In cells cultured at pHe 6.8, ∼30% of telomeres lacked detectable TRF2 (Figure 4C and D). Furthermore, these TRF2-negative telomeres are significantly shorter (on average) than telomeres co-hybridizing with TRF2 ($P < 0.0001$) (Figure 4E).

Telomerase is preferentially recruited to short telomeres

It has been proposed that Cajal bodies promote telomerase assembly and deliver telomerase holoenzyme to telomeres (33–34). Interestingly, western blot showed that the abundance of coilin, a core protein in Cajal Bodies, was lower in cells cultured at pHe 6.8 than in cells cultured at pHe 7.1 or 7.4 (Figure 5A). Consistent with this result, fewer Cajal bodies were detected by IF studies of cells grown at pHe 6.8 (Supplementary Figure S6A). hTR, a RNA component of telomerase, co-localized with Cajal bodies in cells grown at pHe 7.4 and pHe 6.8, suggesting that normal function of Cajal bodies under these pHes (Supplementary Figure S6B).

However, Cajal bodies colocalized with the telomeres in 22% cells cultured at pHe 7.4, while these foci were detected in only 13% of cells grown at pHe 6.8 (Figure 5B and C). When these foci were co-stained with TRF2 (i.e. coilin (blue), TRF2 (green) and telomere DNA probe (red)) (Supplementary Figure S7A), we found that at pHe 6.8, ∼70% of Cajal bodies colocalized with telomeres (CB-occupied telomeres) do not stain with anti-TRF2, whereas no such foci (CB colocalized with TRF2 negative telomere) were detected in cells grown at pHe 7.4 (Supplementary Figure S7B). This suggests that Cajal bodies are preferentially recruited to TRF2-negative telomeres in cells grown at pHe 6.8. We then measured the lengths (RTL in FISH) of CB-occupied telomeres and compared them with the average length of total telomeres in cells (CB-occupied plus CB-free

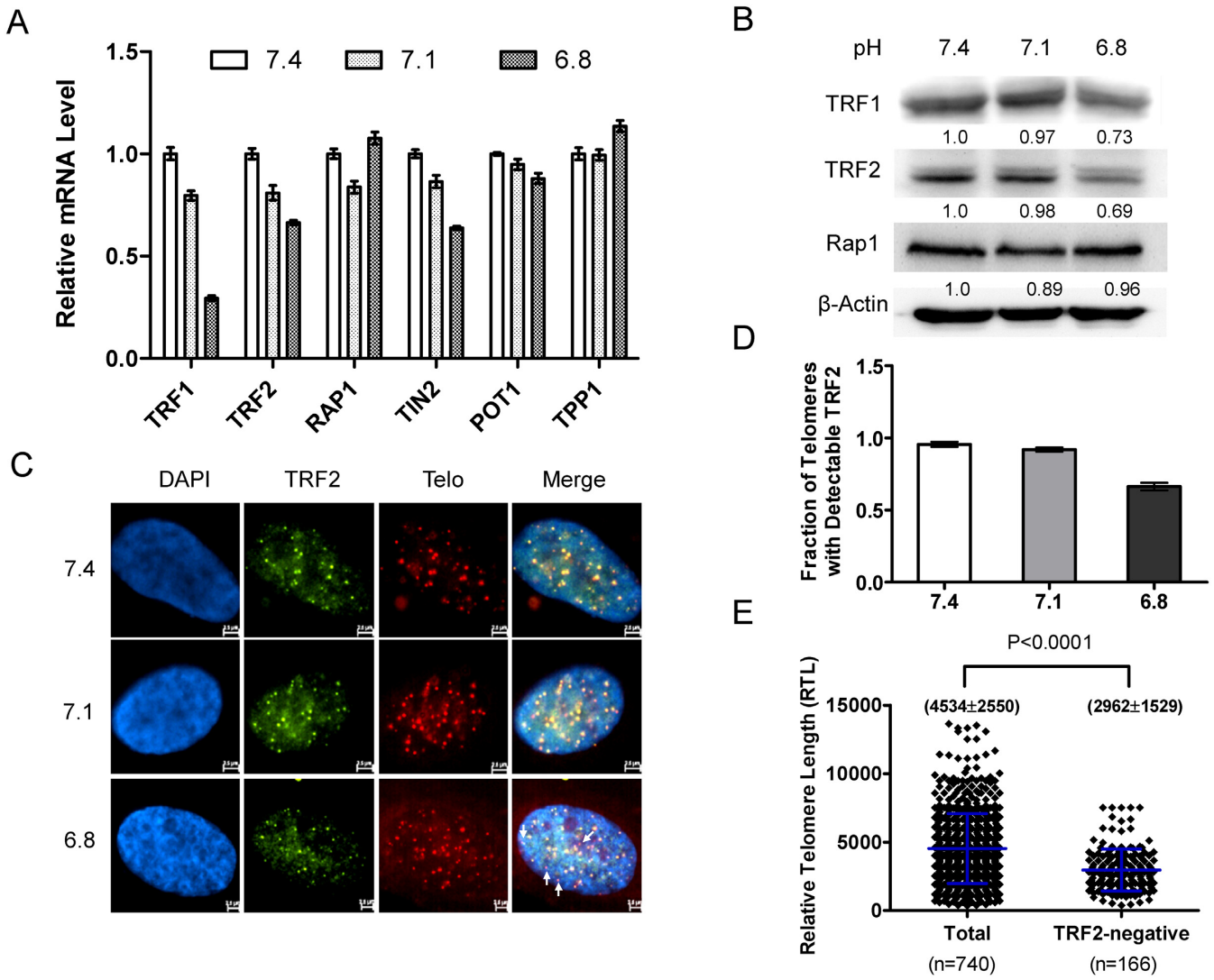

Figure 4. Detection of TRF2-negative telomeres in cells cultured at pHe 6.8. (**A**) q-PCR of shelterin proteins as indicated. Values are average ±SD of three independent experiments. (**B**) Western blot for TRF1, TRF2 and Rap1 in cells grown at the indicated pHe. Bands were quantified by ImageQuant (GE) and normalized to the amount at pH 7.4. The fold of change was indicated below the band. (**C**) Representative images of TRF2-nagative telomeres. TRF2 was visualized by IF; telomeric DNA was visualized by FISH. TRF2-negative telomeres are indicated by arrows. (**D**) Fraction of telomeres lacking detectable TRF2 was calculated. Data shown are average values ±SD of three independent experiments (over 250 telomeres were counted each time). (**E**) Average telomere length of TRF2-negative telomeres and average telomere length in cells (TRF2-positive plus TRF2-negative telomeres). *P*-value was calculated using the Student's *t*-test.

telomeres). The results showed that CB-occupied telomeres are shorter than average length of total telomeres in cells grown at pHe 6.8 ($P < 0.0001$), while no difference was observed in cells grown at pHe 7.4 ($P = 0.6621$) (Supplementary Figure S7C). Altogether, these data strongly support that telomerase is preferentially recruited by Cajal bodies to short telomeres that lack detectable TRF2 in cells grown at pHe 6.8.

It has been reported that during S phase some telomerase RNA, which is believed to represent telomerase, appears in small nucleoplasmic foci that do not co-stain with anti-coilin antibodies (Cajal Bodies) (33). To thoroughly explore the telomerase recruitment at acidic pHe, hTR and telomeres were co-stained in S phase-synchronized cells (Figure 5D). The results showed that hTR-occupied telomeres (telomeres that colocalize with hTR foci) are shorter than average length of total telomeres in cells grown at pHe 6.8 ($P < 0.005$), while no difference was observed in cells grown at pHe 7.4 (Figure 5E). These results demonstrate that telomerase are preferentially recruited to short telomeres in cells cultured at pHe 6.8.

DISCUSSION

Telomere length remains stable over many PDs in telomerase-expressing yeast and human cells grown at neutral pHe by a process known as telomere homeostasis. Under these conditions, human telomerase is recruited to human telomeres in a telomere length-independent manner and almost each telomere is extended by ∼60 nt per cell cycle (16). In contrast, yeast telomerase is active on

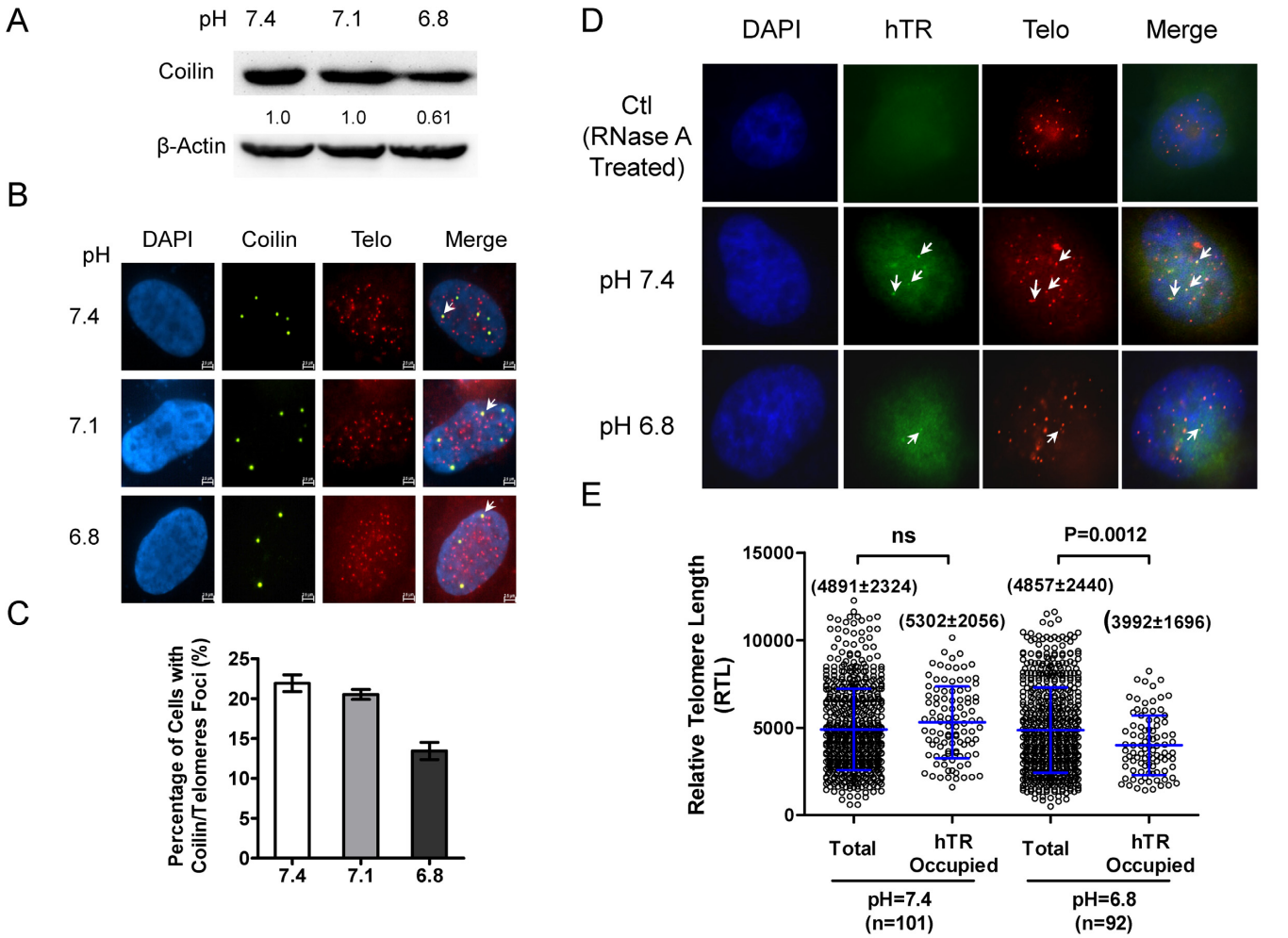

Figure 5. Telomerase is selectively recruited to short telomeres. (**A**) Western blot of coilin in cells grown at indicated pHe. Bands were quantified by ImageQuant (GE) and normalized to the amount at pH 7.4. The fold of change was indicated below the band. (**B**) Cajal bodies and telomeres are visualized by IF and FISH, respectively. Colocalization of Cajal bodies with telomeres is indicated by arrow. (**C**) Quantification of B, values are average ±SD of three independent experiments. (**D**) hTR and telomeres are visualized by RNA and DNA FISH, respectively. S phase-synchronized HeLa cells were co-stained with hTR-probe and telomeric probe. RNase A treated cells were used as a control. (**E**) Quantification of D showing the length (RTL in FISH) of hTR-occupied telomeres (telomeres that colocalize with hTR foci) and average length of total telomeres in cells grown at indicated pHe. Data shown are average values ±SD of four independent experiments. *P*-value was calculated using the Student's *t*-test.

approximately 7% of telomeres per cell cycle, and it adds ≈44 nt onto the telomeric overhang (35). The present study provides evidence that human telomerase can be induced to selectively extend short telomeres by exposure to low pHe (i.e. culture media at pHe 6.8). This finding is of particular interest, because low pHe is characteristic of the hypoxic tumor microenvironment.

It has been found that the shortest telomere, but not average telomere length, is critical for cell viability (36). When a telomere falls below a critical length, the DNA damage response is activated leading to cell apoptosis or senescence. Because of this, telomerase has been considered a valuable therapeutic target in telomerase-expressing tumor cells. If telomerase abundance is low, and it is preferentially recruited to short telomeres in response to low pHe, then inhibition of telomerase could result in short telomere rapidly approaching a critical length that triggers apoptosis or senescence. This generates a strong rationale for research on telomerase-targeted anti-cancer therapeutics. Based on these observations, it is also predicted that anti-telomerase inhibitors will induce cell death in a pHe-dependent manner, so they should be tested in both neutral and slightly acidic cell culture media.

When HeLa cells were cultured at pHe 6.8, the abundance of hTERT and shelterin proteins TRF1/TRF2/TIN2 decreased significantly (Figures 3A and 4A). Interestingly, the knockdown of telomerase by ∼50% causes uniform shortening of telomeres (Figure 3E), rather than selective shortening of long telomeres; therefore, low abundance of telomerase is insufficient to account for preferential extension of short telomeres, as observed in Figure 1D and E. Furthermore, the epigenetic and heterochromatic state of telomeric DNA is not affected by exposure to slightly acidic pHe (Supplementary Figure S4), ruling out the possibility that epigenetics or heterochromatization plays a role in the response to low pHe. In addition, it is known that shelterin

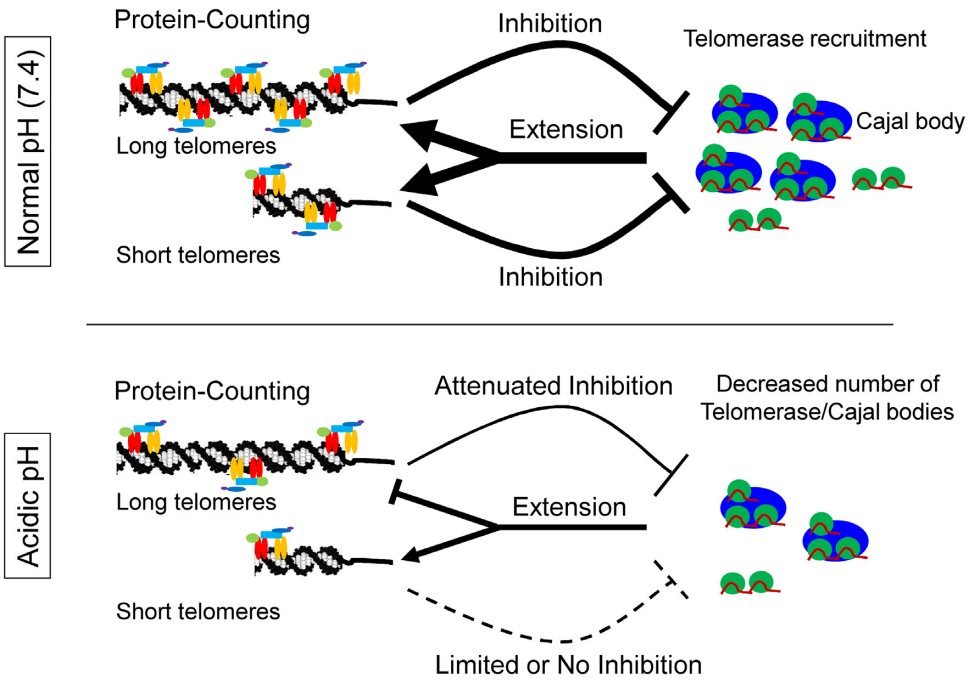

Figure 6. Proposed mechanism by which telomere length, the abundance of telomere-associated shelterin proteins and the abundance of telomerase/Cajal bodies regulate telomerase recruitment, leading to preferential extension of short telomeres (see text for details).

complex or its component serves as a negative player in regulating telomere elongation by telomerase (18), thus decreased number of TRF1, TRF2 and TIN2 would result in telomere elongation rather than observed telomere shortening. Altogether, these results indicated that the preferential extension of short telomeres induced by acidic extracellular pH may involve multiple factors that coordinately regulate telomerase action.

Present data point to the so called 'Protein-counting mechanism' that is well characterized in *Yeast*, but poorly understood in mammalian cells (12). According to this model, cell 'counts' the number of shelterin protein on telomeres, so that telomeres with higher number of shelterin protein have lower opportunity to be extended by telomerase. There are two hypotheses about how this mechanism might work: the first hypothesis suggests that telomere lengthening is regulated by preferential recruitment of telomerase to short telomeres; the second hypothesis suggests that telomerase exists in an inactive or active state, such that it is inactive on long telomeres and active on short telomeres (35). Although these hypotheses are not fully exclusive, the results presented here support the first hypothesis. The present study shows that the amount of TRF1 and TRF2 decrease significantly at pHe 6.8, such that up to 30% of telomeres appear to be TRF2-negative (Figure 4), and that TRF2-negative telomeres are shorter than the average telomere length in cells. Furthermore, at pHe 6.8, the abundance of coilin, a marker of Cajal bodies, decreases. The decreased number of TRF2/shelterin on the shorter telomeres is predicted to stimulate recruitment of telomerase, which is consistent with results shown in Figure 5 and Supplementary Figure S7. Based on the current data and our previous results (14,16), we propose the following model: when telomerase and Cajal bodies are abundant, inhibition by shelterin and extension by telomerase remain in equilibrium, ensuring that most telomeres can be extended by telomerase (Figure 6). However, in response to slightly acidic pHe, the abundance of shelterin complex and telomerase/Cajal bodies decrease. Long telomeres may harbor reduced but still substantial inhibitory units (shelterin complex), but short telomeres become TRF2/shelterin-deficient and they preferentially recruit telomerase/Cajal bodies (Figure 6). The present study provides a new insight into our understanding of mechanisms that regulate telomerase action in human cells, and may facilitate development of effective telomerase-targeted anti-cancer therapies.

SUPPLEMENTARY DATA

Supplementary Data are available at NAR Online.

ACKNOWLEDGEMENT

We thank Dr Michael Terns at university of Georgia for providing RNA/DNA FISH protocol.

FUNDING

National Natural Science Foundation of China [31271472; 31322033; 31301110]; National Basic Research Program of China [2014CB964703]; Guangdong Province Higher Vocational Colleges & Schools; Pearl River Scholar Funded Scheme (2013). Funding for open access charge: National Natural Science Foundation of China Grants [31571410].
Conflict of interest statement. None declared.

REFERENCES

1. Konerding,M.A., Malkusch,W., Klapthor,B., van Ackern,C., Fait,E., Hill,S.A., Parkins,C., Chaplin,D.J., Presta,M. and Denekamp,J. (1999) Evidence for characteristic vascular patterns in solid tumours: quantitative studies using corrosion casts. *Br. J. Cancer*, **80**, 724–732.
2. Ngo,D.C., Ververis,K., Tortorella,S.M. and Karagiannis,T.C. (2015) Introduction to the molecular basis of cancer metabolism and the Warburg effect. *Mol. Biol. Rep.*, **42**, 819–823.
3. Gerweck,L.E. and Seetharaman,K. (1996) Cellular pH gradient in tumor versus normal tissue: potential exploitation for the treatment of cancer. *Cancer Res.*, **56**, 1194–1198.
4. Vaupel,P., Kallinowski,F. and Okunieff,P. (1989) Blood flow, oxygen and nutrient supply, and metabolic microenvironment of human tumors: a review. *Cancer Res.*, **49**, 6449–6465.
5. Tannock,I.F. and Rotin,D. (1989) Acid pH in tumors and its potential for therapeutic exploitation. *Cancer Res.*, **49**, 4373–4384.
6. Gillies,R.J., Raghunand,N., Karczmar,G.S. and Bhujwalla,Z.M. (2002) MRI of the tumor microenvironment. *J. Magn. Reson. Imaging*, **16**, 430–450.
7. Griffiths,J.R., Stevens,A.N., Iles,R.A., Gordon,R.E. and Shaw,D. (1981) 31P-NMR investigation of solid tumours in the living rat. *Biosci. Rep.*, **1**, 319–325.
8. Kallinowski,F., Schlenger,K.H., Runkel,S., Kloes,M., Stohrer,M., Okunieff,P. and Vaupel,P. (1989) Blood flow, metabolism, cellular microenvironment, and growth rate of human tumor xenografts. *Cancer Res.*, **49**, 3759–3764.
9. Stubbs,M., McSheehy,P.M., Griffiths,J.R. and Bashford,C.L. (2000) Causes and consequences of tumour acidity and implications for treatment. *Mol. Med. Today*, **6**, 15–19.
10. Greider,C.W. and Blackburn,E.H. (1985) Identification of a specific telomere terminal transferase activity in Tetrahymena extracts. *Cell*, **43**, 405–413.
11. Kim,N.W., Piatyszek,M.A., Prowse,K.R., Harley,C.B., West,M.D., Ho,P.L., Coviello,G.M., Wright,W.E., Weinrich,S.L. and Shay,J.W. (1994) Specific association of human telomerase activity with immortal cells and cancer. *Science*, **266**, 2011–2015.
12. Bianchi,A. and Shore,D. (2008) How telomerase reaches its end: mechanism of telomerase regulation by the telomeric complex. *Mol. Cell*, **31**, 153–165.
13. Ouellette,M.M., Liao,M., Herbert,B.S., Johnson,M., Holt,S.E., Liss,H.S., Shay,J.W. and Wright,W.E. (2000) Subsenescent telomere lengths in fibroblasts immortalized by limiting amounts of telomerase. *J. Biol. Chem.*, **275**, 10072–10076.
14. Zhao,Y., Abreu,E., Kim,J., Stadler,G., Eskiocak,U., Terns,M.P., Terns,R.M., Shay,J.W. and Wright,W.E. (2011) Processive and distributive extension of human telomeres by telomerase under homeostatic and nonequilibrium conditions. *Mol. Cell*, **42**, 297–307.
15. Samper,E., Flores,J.M. and Blasco,M.A. (2001) Restoration of telomerase activity rescues chromosomal instability and premature aging in Terc-/- mice with short telomeres. *EMBO Rep.*, **2**, 800–807.
16. Zhao,Y., Sfeir,A.J., Zou,Y., Buseman,C.M., Chow,T.T., Shay,J.W. and Wright,W.E. (2009) Telomere extension occurs at most chromosome ends and is uncoupled from fill-in in human cancer cells. *Cell*, **138**, 463–475.
17. Diolaiti,M.E., Cimini,B.A., Kageyama,R., Charles,F.A. and Stohr,B.A. (2013) In situ visualization of telomere elongation patterns in human cells. *Nucleic Acids Res.*, **41**, e176.
18. Palm,W. and de Lange,T. (2008) How shelterin protects mammalian telomeres. *Annu. Rev. Genet.*, **42**, 301–334.
19. Smogorzewska,A., van Steensel,B., Bianchi,A., Oelmann,S., Schaefer,M.R., Schnapp,G. and de Lange,T. (2000) Control of human telomere length by TRF1 and TRF2. *Mol. Cell. Biol.*, **20**, 1659–1668.
20. Ye,J.Z. and de Lange,T. (2004) TIN2 is a tankyrase 1 PARP modulator in the TRF1 telomere length control complex. *Nat. Genet.*, **36**, 618–623.
21. Loayza,D. and De Lange,T. (2003) POT1 as a terminal transducer of TRF1 telomere length control. *Nature*, **423**, 1013–1018.
22. Ye,J.Z., Hockemeyer,D., Krutchinsky,A.N., Loayza,D., Hooper,S.M., Chait,B.T. and de Lange,T. (2004) POT1-interacting protein PIP1: a telomere length regulator that recruits POT1 to the TIN2/TRF1 complex. *Genes Dev.*, **18**, 1649–1654.
23. McBrian,M.A., Behbahan,I.S., Ferrari,R., Su,T., Huang,T.W., Li,K., Hong,C.S., Christofk,H.R., Vogelauer,M., Seligson,D.B. *et al.* (2013) Histone acetylation regulates intracellular pH. *Mol. Cell*, **49**, 310–321.
24. Chen,Y., Deng,Z., Jiang,S., Hu,Q., Liu,H., Songyang,Z., Ma,W., Chen,S. and Zhao,Y. (2015) Human cells lacking coilin and Cajal bodies are proficient in telomerase assembly, trafficking and telomere maintenance. *Nucleic Acids Res.*, **43**, 385–395.
25. Chai,W., Du,Q., Shay,J.W. and Wright,W.E. (2006) Human telomeres have different overhang sizes at leading versus lagging strands. *Mol. Cell*, **21**, 427–435.
26. Huang,J., Wang,F., Okuka,M., Liu,N., Ji,G., Ye,X., Zuo,B., Li,M., Liang,P., Ge,W.W. *et al.* (2011) Association of telomere length with authentic pluripotency of ES/iPS cells. *Cell Res.*, **21**, 779–792.
27. Abreu,E., Aritonovska,E., Reichenbach,P., Cristofari,G., Culp,B., Terns,R.M., Lingner,J. and Terns,M.P. (2010) TIN2-tethered TPP1 recruits human telomerase to telomeres in vivo. *Mol. Cell Biol.*, **30**, 2971–2982.
28. Abreu,E., Terns,R.M. and Terns,M.P. (2011) Visualization of human telomerase localization by fluorescence microscopy techniques. *Methods Mol. Biol.*, **735**, 125–137.
29. Wu,P. and de Lange,T. (2008) No overt nucleosome eviction at deprotected telomeres. *Mol. Cell. Biol.*, **28**, 5724–5735.
30. Webb,B.A., Chimenti,M., Jacobson,M.P. and Barber,D.L. (2011) Dysregulated pH: a perfect storm for cancer progression. *Nat. Rev. Cancer*, **11**, 671–677.
31. Benetti,R., Garcia-Cao,M. and Blasco,M.A. (2007) Telomere length regulates the epigenetic status of mammalian telomeres and subtelomeres. *Nat. Genet.*, **39**, 243–250.
32. Garcia-Cao,M., O'Sullivan,R., Peters,A.H., Jenuwein,T. and Blasco,M.A. (2004) Epigenetic regulation of telomere length in mammalian cells by the Suv39h1 and Suv39h2 histone methyltransferases. *Nat. Genet.*, **36**, 94–99.
33. Tomlinson,R.L., Ziegler,T.D., Supakorndej,T., Terns,R.M. and Terns,M.P. (2006) Cell cycle-regulated trafficking of human telomerase to telomeres. *Mol. Biol. Cell*, **17**, 955–965.
34. Zhu,Y., Tomlinson,R.L., Lukowiak,A.A., Terns,R.M. and Terns,M.P. (2004) Telomerase RNA accumulates in Cajal bodies in human cancer cells. *Mol. Biol. Cell*, **15**, 81–90.
35. Teixeira,M.T., Arneric,M., Sperisen,P. and Lingner,J. (2004) Telomere length homeostasis is achieved via a switch between telomerase- extendible and -nonextendible states. *Cell*, **117**, 323–335.
36. Hemann,M.T., Strong,M.A., Hao,L.Y. and Greider,C.W. (2001) The shortest telomere, not average telomere length, is critical for cell viability and chromosome stability. *Cell*, **107**, 67–77.